Uncertainty in 3D gel dosimetry

Yves De Deene[1,2] and Andrew Jirasek[3,4]
[1]Dept. of Engineering, Faculty of Science, Macquarie University, Sydney, Australia
[2]Institute of Medical Physics, School of Physics, University of Sydney
[3]Physics, I.K. Barber School of Arts and Science, University of British Columbia, Okanagan Campus, Canada
[4]Dept. Physics and Astronomy, University of Victoria, Canada

E-mail: yves.dedeene@mq.edu.au, andrew.jirasek@ubc.ca

Abstract. Three-dimensional (3D) gel dosimetry has a unique role to play in safeguarding conformal radiotherapy treatments as the technique can cover the full treatment chain and provides the radiation oncologist with the integrated dose distribution in 3D. It can also be applied to benchmark new treatment strategies such as image guided and tracking radiotherapy techniques. A major obstacle that has hindered the wider dissemination of gel dosimetry in radiotherapy centres is a lack of confidence in the reliability of the measured dose distribution. Uncertainties in 3D dosimeters are attributed to both dosimeter properties and scanning performance. In polymer gel dosimetry with MRI readout, discrepancies in dose response of large polymer gel dosimeters versus small calibration phantoms have been reported which can lead to significant inaccuracies in the dose maps. The sources of error in polymer gel dosimetry with MRI readout are well understood and it has been demonstrated that with a carefully designed scanning protocol, the overall uncertainty in absolute dose that can currently be obtained falls within 5% on an individual voxel basis, for a minimum voxel size of 5 mm^3. However, several research groups have chosen to use polymer gel dosimetry in a relative manner by normalizing the dose distribution towards an internal reference dose within the gel dosimeter phantom. 3D dosimetry with optical scanning has also been mostly applied in a relative way, although in principle absolute calibration is possible. As the optical absorption in 3D dosimeters is less dependent on temperature it can be expected that the achievable accuracy is higher with optical CT. The precision in optical scanning of 3D dosimeters depends to a large extend on the performance of the detector. 3D dosimetry with X-ray CT readout is a low contrast imaging modality for polymer gel dosimetry. Sources of error in x-ray CT polymer gel dosimetry (XCT) are currently under investigation and include inherent limitations in dosimeter homogeneity, imaging performance, and errors induced through post-acquisition processing. This overview highlights a number of aspects relating to uncertainties in polymer gel dosimetry.

1. Introduction

1.1. 3D dose verification with integrating dosimeters

3D radiation dosimetry provides a unique ability to display dose distributions occurring in clinical radiotherapy in three dimensions (3D) in humanoid shaped phantoms [1-3]. It has a unique role to play in safeguarding conformal radiotherapy treatments, as it is the only dosimeter that covers the whole treatment chain and provides the radiation oncologist with the integrated dose distribution in 3D.

Moreover, 3D dosimeters can also be used to benchmark motion compensation radiotherapy technologies when mounted in a motion phantom. However, some doubts with respect to the overall reliability have overshadowed the wider dissemination of 3D radiation dosimetry in radiation centers.

1.2. 'Absolute' versus 'relative' 3D dosimetry

Although the terminology 'absolute' and 'relative' is somewhat ill defined in gel literature, we use the term 'absolute' to describe the approach where an independent external calibration of the 3D dosimeter is applied in contrast to the term 'relative' 3D dosimetry, where the 3D dose distribution is normalized towards some internal reference points (mostly the dose in the isocentre and the dose in a low or high dose region).

When utilizing polymer gels with MRI readout, significant differences in dose-R_2 response have been found between different 3D dosimeters that were poured in small calibration vials as compared to larger phantom recipients [4, 5]. This finding severely compromises the use of an externally derived calibration curve to convert the measured R_2 maps to dose maps. Several possible reasons have been proposed as explanation for the observed discrepancies such as differences in cooling rate [6], changes in temperature during irradiation as a result of the exothermal radiation induced polymerization reaction [7] and physicochemical changes related to an oxygen-antioxidant imbalance [8]. To circumvent the discrepancies in dose-R_2 response between small test tubes and larger volumetric anthropomorphic gel dosimeter phantoms, many researchers have chosen to apply an internal calibration (i.e. the R_2 is calibrated to dose by using two points within the phantom as 'known' doses), which is further referred to as 'relative' dosimetry. Regardless the fact that with an internal calibration, the ability of gel dosimetry to safeguard absolute dose information of a treatment is lost, it should also be emphasized that there is a potentially more severe danger with this strategy because the mentioned mechanisms may depend on radiation dose, dose rate, environmental conditions and size and shape of the phantom. Most often, a linear calibration curve is assumed with this approach. There is therefore no evidence that the same mechanism for the observed discrepancies would not cause any dose measurement errors within the volumetric polymer gel dosimeter phantom itself. Indeed, a major source of these discrepancies is attributed to temperature differences during scanning within the volumetric dosimeter phantom.

3D dosimetry using optical readout has mostly been performed with relative or internal calibration, although there doesn't seem to be a specific argument why absolute calibration could not be performed. The radiation absorptivity defined as absorption per unit of distance per dose should only depend on the dosimeter material and calibration samples can be exposed to known radiation doses and either scanned or readout using a benchtop optical spectrometer. Studies are underway to determine the uncertainty associated with external dose calibration of dye based plastic dosimeters.

Early investigations using x-ray CT polymer gel dosimetry (PGD) utilized linear calibration curves and "relative" dosimetry [9, 10] Calibrations were performed either in a purely relative sense (assuming a known dose at a given point) or via large phantom irradiation with small fields of known doses. However, calibration phantoms were not designed to match test (anthropomorphic) phantoms, thus introducing potential errors within the calibration procedure. Since those early experiments, refinements to the overall calibration procedure in x-ray CT PGD have been made. As in the case with MRI, it has been recognized that small vial irradiations can not be used to calibrate large test phantoms due to the differing response between small and large PGD samples. As mentioned above, this observation points to the differential response being due to properties of the gel reaction (exothermic etc) as opposed to an imaging modality-based explanation. Furthermore, it has been shown that a linear dose response can not be assumed when utilizing high dose-sensitivity polymer gel with x-ray CT imaging [11, 12]. Recent experiments have shown that when utilizing a non linear calibration curve obtained from the irradiation of a portion of the test phantom with a known dose distribution, absolute dosimetry can be performed which results in a dose dependent accuracy and precision, as described in further detail below.

1.3. Evaluating the uncertainty of 3D dosimetry

The evaluation methods that have been applied by many 3D dosimetry research groups to give evidence of the 'potential' of 3D dosimeters are often based on a percentage number of voxels that pass gamma criteria between a measured dose distribution and a treatment planning system (TPS) calculated dose distribution. This value of pass rates obviously depends on the number of slices and the size (field-of-view) of the dose maps taken into consideration. Some have suggested to use a dose threshold in which gamma is calculated but even in this case, care must be taken in using gamma pass rates that will still depend on the topological 'complexity' of the dose distribution. Although it is recognized that gamma maps are a valuable tool in benchmarking a radiotherapy treatment plan, the use of a percentage value of passing pixels in benchmarking a dosimetry technique against a TPS calculated dose distribution can be misleading as proof of the reliability of the dosimetry technique. Gamma map analysis should also be performed with much care as the measured dose distributions may contain stochastic noise. Gamma values may be significantly underestimated when the evaluated dose distribution contains noise [13]. Moreover, it is not beyond discussion to what extend a TPS calculated dose distribution should be used as 'golden standard' to benchmark a new dosimeter. Of course, it is recognized that the intrinsic problem with the benchmarking of a 3D dosimeter is that there does not exist another 3D dosimetric 'golden standard' to compare against. The most reasonable strategy is to compare doses obtained with gel dosimetry with doses obtained by the most reliable dosimetry techniques that apply to a certain spatial dimension. For example, dose profiles of a single field (photons and electrons) can be compared with dose profiles obtained with an ionization chamber or diamond detector [14, 15]. In two dimensions, 3D dosimetry can be compared with film dosimetry [3, 14, 16]. Dose distributions obtained with 3D dosimetry have been compared with those calculated with treatment planning software [3, 17-23]. Errors that compromise the accuracy may occur at different stages of the dosimetry procedure [24]. Given the uncertainties with respect to the calibration, we argue that a more stringent approach using other dosimeters and treatment planning should be applied to benchmark 3D radiation dosimetry than a gamma evaluation against a single treatment plan.

1.4. Accuracy and precision

Accuracy is defined as the degree of conformity of a measured or calculated quantity (a measurand) to its actual (true) value. *Precision* is defined as the ability of a measurement to be consistently reproduced. Accuracy and precision can be defined statistically in terms of the deviation of the mean value from the reference value and the standard deviation of the mean value of many measurements respectively (figure 1). The measurement uncertainty of a single experiment thus comprises both systematic and random errors. Uncertainties have further been classified in type A and type B uncertainties where type A standard uncertainty is obtained from a probability density function derived from an observed frequency distribution, while type B standard uncertainty is obtained from an assumed probability density function that is based on the degree of belief that an event will occur.

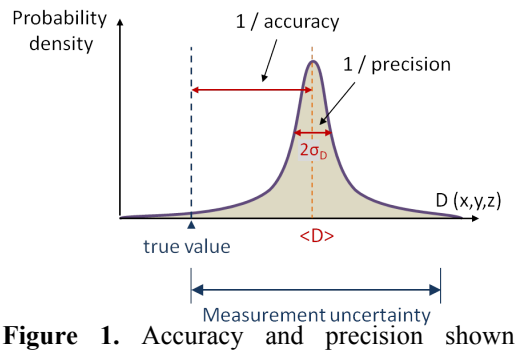

Figure 1. Accuracy and precision shown schematically in terms of probabilities of occurrence. Precision can be characterised in terms of the standard deviation of many measurements (experiments). The accuracy is characterized by the deviation of the mean of many measurements from the reference (known) value.

In the case of 3D radiation dosimetry, uncertainty applies to both dose and space. In a gel dosimetry dose verification experiment (and any radiation treatment), the spatial and dosimetric dimensions are interwoven. For large volume dosimeters it is theoretically impossible to extract both dosimetric and spatial errors from a measured spatial dose distribution (i.e. the result of a 3D gel dosimetry experiment). To comprise both spatial and dosimetric

performance in one parameter, Low *et al* have introduced the gamma-index [25]. Other dose distribution comparisons are performed on the basis of maximum allowed dose differences [26].

The overall uncertainty of 3D radiation dosimetry can be achieved through a reproducibility study of the complete dosimetry experiment from gel fabrication to dose distribution analysis. An extensive reproducibility study, comprising the repetition of a gel dosimetry experiment has been carried out for polymer gel dosimeters with MRI readout [27]. It is imperative to realize that in a clinical verification with gel dosimetry, consisting of a single experiment, the uncertainty of the dose measured in each voxel comprises both the systematic inaccuracy and random errors, including stochastic image noise.

A typical clinical 3D dose verification experiment is performed in different steps and errors can occur at each stage (figure 2): (1) The polymer gel dosimeter is fabricated in a chemical laboratory and is stored until radiation. Any deviations in the chemical composition through inhomogeneous mixing, remnant impurities in the gel container or oxygen permeability within the gel containers can give rise to discrepancies between calibration and volumetric phantoms [8]. Moreover, a difference in temperature course during storage may also affect the dose-R2 response between calibration and test phantoms [6]. Most of these deviations are compensated for by using calibration phantoms that are (i) fabricated from the same batch of gel, (ii) of the same material composition, and (iii) of similar volumes. (2) The gel dosimeter phantom is then scanned with CT and a treatment plan is devised (3) on the CT images, resulting in a virtual planning target volume (PTV) and a set of critical organs. At this stage, just as with a patient, a reference coordinate system is allocated to the phantom by use of marker lines that are drawn on the phantom. In addition, for co-registration of the dose maps with the TPS, stereotactic fixtures or fiducial markers [28] can be placed on the phantom that will later be visible on the imaging modality of interest (MRI, optical CT, x-ray CT). Positional setup errors are likely to result in deviations between the planned and the measured dose distribution. These deviations are not intrinsic to the gel dosimeter but are indicative for errors that may occur during the actual patient treatment. (4) Upon irradiation, a complex set of radiation-induced chemical reactions take place. On a molecular level, these reactions are probabilistic in nature but on the spatial scale of clinical dose verification experiments, this radiochemical noise is insignificant.

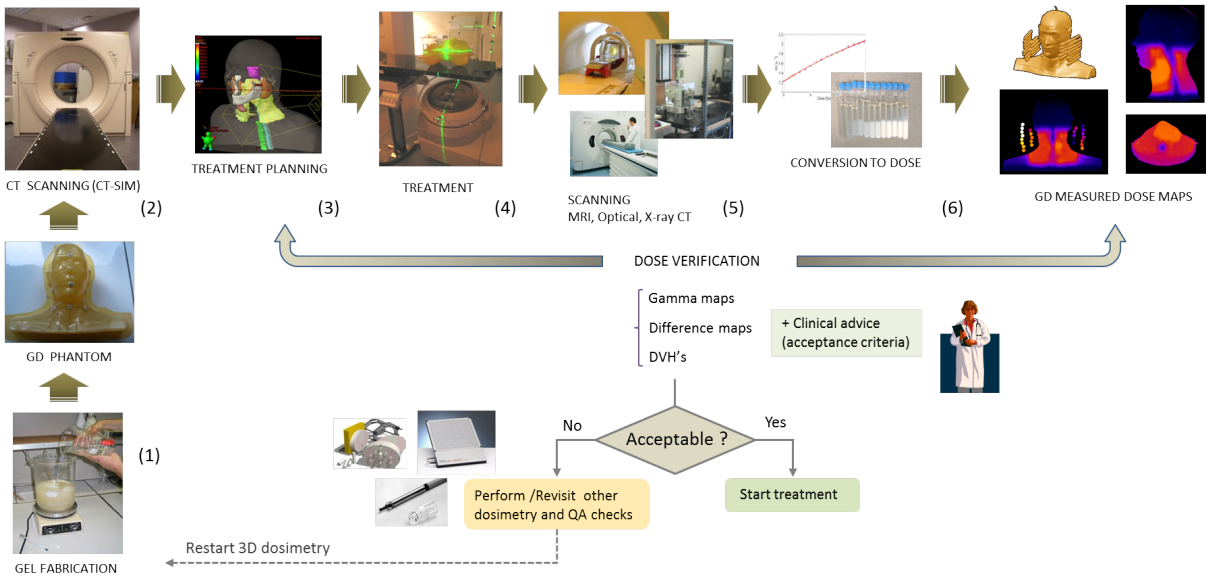

Figure 2. In a clinical dose verification experiment with 3D dosimetry, the dosimeter phantom is taken through the entire treatment chain. Possible dosimetric or setup errors can occur at the different stages. 3D dosimetry fulfills an important role in benchmarking the complete treatment chain.

Any positional set-up errors in treatment with respect to the planned treatment will affect the dose distribution. This error may also occur in patient treatment and is therefore not intrinsic to 3D dosimetry. In benchmarking 3D radiation dosimetry however, the experimental set-up error should be minimized as much as possible by adequate positioning aids in order to isolate the other error sources. Other sources of deviation in dose reading that may occur during irradiation of the gel dosimeter are related to the dependence of the irradiation response on the temperature of the 3D dosimeter during irradiation, on the dose rate and on the energy spectrum of the irradiation beam [29, 31]. It is important to realize that differences in dose rate (and energy) will occur in the irradiated 3D volume even if the photon fluence rate (in terms of MU/min) of the individual beams is kept constant. Another important characteristic of the dosimeter is its temporal and spatial integrity [32, 33]. These errors are inherent to the dosimeter material and should be minimized as they compromise the specificity of the dosimeter. After irradiation, the gel dosimeter is imaged (MRI, optical CT, x-ray CT) (5). During imaging, image noise will add to the measurements. In order to minimize the noise in the measured dose distribution the scanning parameters should be optimized [34-36]. The processing (fitting, filtering etc) of acquired data (6), may have a significant influence on the amplification of noise inherent in the data. For example, in quantitative R_2-NMR scanning it is found that a least-square fit will amplify the thermal noise in the base images to a larger extent than a chi-square (χ^2) based minimization. Imaging artifacts may result in systematic errors both dosimetric and spatially. A classification of the error sources in Type A and B uncertainties can be found elsewhere [37].

2. Uncertainties in polymer gel dosimetry with MRI readout

The overall dosimetric precision is compromised by random errors in the different operations (figure 2) carried out in the dosimetry experiment. The first step in a gel dosimetry experiment is weighting the chemicals. Stochastic variations in the weighting will result in variations in the measured dose-related value (R_1, R_2, MT) as the dose-response is determined by the chemical composition. It is found that other manufacturing conditions may also have an influence on the dose-response such as the temperature during fabrication and the oxygen concentration in the gel dosimeter. Stochastic variations in the controlled temperature between different experiments will therefore also lead to variations in the measured dose-related value. These variations only contribute to the overall uncertainty of the dosimeter if their contribution is different between the calibration phantom and the 3D dosimeter phantom, e.g. as a result of different cooling rates of small phantoms as compared to large phantoms. When gel dosimeters are handled under conditions of good practice [37], the physico-chemical mechanisms should not contribute to more than a total error of 2% in the dose measurement [38]. It is paramount that in some gel dosimeters (such as MAGAT) where a significant dose rate dependence is found [29], the figure of uncertainty may be exceeded.

Also during irradiation there are different sources of stochastic variable contributions that determine the overall dosimetric precision such as variations in the dose delivery, variations in the temperature during irradiation [29, 30] and stochastic variations in the positioning of the calibration phantoms. Similar factors of chemical and irradiation uncertainty are also present with optical and X-ray CT but their respective contribution may be different.

MR images of the gel dosimeter will contain noise in the images as a result of thermal detector and phantom noise. This noise component will propagate into the derived quantitative MR images. The noise contribution is also determined by some scan parameters that can be optimized to achieve a maximum precision [34, 35]. In gel dosimetry with MRI readout, a calibration of the scanned parametric map (e.g. R_2 map) is needed to obtain a dose map. The stochastic noise in the dose maps can be kept well below 0.8% standard deviation, resulting in a maximum deviation of 2.4% on an individual voxel basis with a confidence of 99% [24]. It is worth noting that the values mentioned here for thermal image noise are for imaging voxels with a volume of 3 mm^3 and can be proportionally reduced by scaling to a grid size similar to the treatment plan. Any random errors that operate on the calibration samples will also affect the uncertainty of the dose map. In addition, the stochastic variations in beam output during radiation of the calibration vials can also be assumed to be

significantly less than 1% that is also supported by a reproducibility study where 20 (calibration) samples were irradiated with the same dose and under the same conditions. The resulting type A (random) uncertainty on the individual voxel level is therefore considered as predominantly originating from thermal noise during scanning.

Systematic errors (type B uncertainty) during MRI scanning of gel dosimeters are attributed to: B_0 and B_1-field non-uniformities; gradient non-uniformities; and temperature differences between calibration phantoms and volumetric dosimeter phantom [40-45]. Scanner related sources of uncertainty may be kept well below 3% by a proper scanning setup and/or by applying post-processing compensation methods such as for B_0- and B_1-field non-uniformity [2, 46]. A source of uncertainty that has a significant contribution to the overall uncertainty is related to temperature deviations and variations during scanning [39]. These effects can be minimized by use of an imaging sequence with centric k-space reordering [44] and/or an active temperature stabilization using thermal pads or a temperature stabilized water reservoir. An extensive set of guidelines on how to scan polymer gel dosimeters with MRI has been discussed in previous conference proceedings [37, 47].

3. Uncertainties in 3D dosimetry with optical readout

Different optical scanner prototypes [48-60] have been developed to scan 3D dosimeters. As with MRI scanning of 3D dosimeters, the uncertainties are determined by the combination of the dosimeter characteristics and the optical scanner, which are often coupled and can't be separated easily. For example, sensitivity to light scatter varies between scanner designs. As a result, the contribution of the uncertainty caused by light scattering in polymer gel dosimeters will depend on the scanner type.

For polymer gel dosimeters, the same physico-chemical sources of uncertainties, as discussed in section 2, apply. It has also been found that variations in the fabrication process and chemical composition in both micelle gel dosimeters [61, 62] and plastic dosimeters such as PRESAGE [63-65] and Flexydos3D [66] result in inter-batch differences in the optical dose response. Although it is expected that intra-batch variations are minimal, until now, their effect on the uncertainty as a result of physico-chemical differences between calibration samples and volumetric dosimeter phantoms has not been investigated. Temperature dependence during irradiation in the order of 2% per degree Celsius has been detected in both PRESAGE [63, 64] and micelle gel dosimeters [62]. The Flexydos3D dosimeters are still under investigation.

Detector noise will also contribute to pixel-by-pixel type A dose uncertainty. For CCD cameras, there is a square root relation between the noise and the signal intensity [67]. The propagation of noise from the detector noise to the signal-to-noise ratio (SNR) in the reconstructed optical density images can be easily simulated [67, 68]. It is found that the SNR in the reconstructed images also depends on the spatial frequency filter that is applied in the reconstruction algorithm. Computational simulations on synthetic phantoms can also be applied to detect the effect of the reconstruction algorithm on the modulation transfer function (MTF) and, hence, the spatial uncertainty introduced by the reconstruction [67, 68]. The spatial uncertainty can also be determined experimentally by using adequate resolution phantoms [54]. The SNR and the dynamic range of the detector are performance characteristics of the detector and are often associated with its cost. Just as with any other readout system, the SNR in the dose maps can be improved by averaging out several images at the cost of measurement time. The optimal dose range of the dosimeter is also determined by the SNR characteristics of the optical scanner, including both the detector noise performance and the reconstruction algorithm.

Systematic errors (type B uncertainty) during optical scanning may affect both the spatial and dose accuracy and are related to imaging artefacts that can be both scanner related or phantom related. Phantom related artefacts are caused by refractive index differences between phantom and refractive index matching fluid [55], light scattering [56, 69], refractive index variations in the phantom as a result of convection during the exothermal solidification process [67] and granular impurities such as dust particles in the phantom [72]. Phantom related systematic errors that affect calibration may also originate from temperature differences during irradiation [62-64] and physico-chemical sources of

uncertainty such as temperature dependent auto-oxidation [70] of the leucodye and the effect of oxygen. Scanner related artefacts are scanner specific and can be caused by drift or fluctuations in the light source and/or detector [58, 71, 72], scratches on the optical components [71, 72], internal reflections in the optical components [71, 72], ambient stray light [71], desynchronization between galvanomirror and detector in laser scanners leading to misalignments in the sinogram [58, 72] and off-centric axis alignment with respect to the projections. Ray tracing [52] or Monte-Carlo simulation software [73] can be helpful in describing the performance of the scanner and in optimizing the design to minimize the instrumental uncertainties. Attempts to perform an independent calibration with calibration phantoms have been undertaken [71, 74, 75] but more studies are required to determine the achievable absolute dose accuracy with the various optically sensitive dosimeters. A comprehensive overview of optical scanning and tips-and-tricks can be found in previous conference proceedings [48, 76].

4. Uncertainties in 3D dosimetry with X-ray CT readout

All uncertainties and errors incurred during the PGD manufacture and irradiation steps of figure 2, and described above, are also present when imaging PGDs with x-ray CT. However, certain sensitivities, such as sensitivity to irradiation temperature, are less prevalent than when imaging with MRI. These observations speak to the low contrast resolution that is obtained when using x-ray CT for PGD imaging.

Imaging PGDs with x-ray CT is associated with a distinct host of uncertainties and errors that must be considered within any given experiment. We here subdivide these uncertainties and errors in to two categories: those induced through the imaging procedure; and those induced through post image acquisition processing. Within the imaging procedure, uncertainties within a resultant image are compounded by set-up errors and signal to noise ratio (SNR) considerations through imaging parameter optimization. An attractive feature of x-ray CT PGD is the fact that the CT process is already incorporated into the radiotherapy work-flow. Hence, physical set-up errors can be minimized through the use of standardized immobilization devices that are constant throughout the experiment (from treatment plan CT acquisition through to dose information extraction imaging). With rigorous attention to phantom set-up reproducibility, a ~1mm accuracy in set up can be achieved with an anthropomorphic head phantom and CT mask immobilization. In terms of imaging parameter optimization, work has been reported in the literature outlining the affects of parameter manipulation on resultant image SNR [36]. Image SNR can be optimized through judicious choice of CT parameter acquisition. While SNR can be improved through, essentially increasing the number of photons hitting any given detector, such a scheme comes at the expense of tube load and, therefore, image acquisition time, which is restricted by any required tube cooling.

Post CT imaging, data processing is required to convert raw CT images to high SNR dose maps. Figure 3 illustrates factors affecting systematic and random errors and uncertainties incurred through each processing step. Each step throughout the procedure outlined in figure 3 carries with it an inherent uncertainty which, ultimately, propagates through to the dose calibration function and hence also through to the calibrated dose maps. Recent work has incorporated errors throughout each step in order to obtain an estimation of the accuracy and precision in calibrated CT images. Results show that accuracy and precision throughout the calibration procedure are highly dose dependent and hence a single quantity for accuracy or precision can not be realistically quoted. Minimum errors in accuracy and precision occur in the “mid-dose” regions (~7 – 20 Gy) of the calibration and are quoted in the 5% range. It must also be noted that a non-linear calibration curve was essential in performing the “absolute” calibration in this case. Several non-linear functions were tested and a hyperbolic tangent function was found to provide the highest level of accuracy and precision in the resultant dose maps. This function was found empirically and does not necessarily offer insight in to reaction dynamics within PGDs, although this point has not been investigated in depth. In summary, a linear calibration would result in highly increased errors and is therefore not recommended when performing x-ray CT PGD.

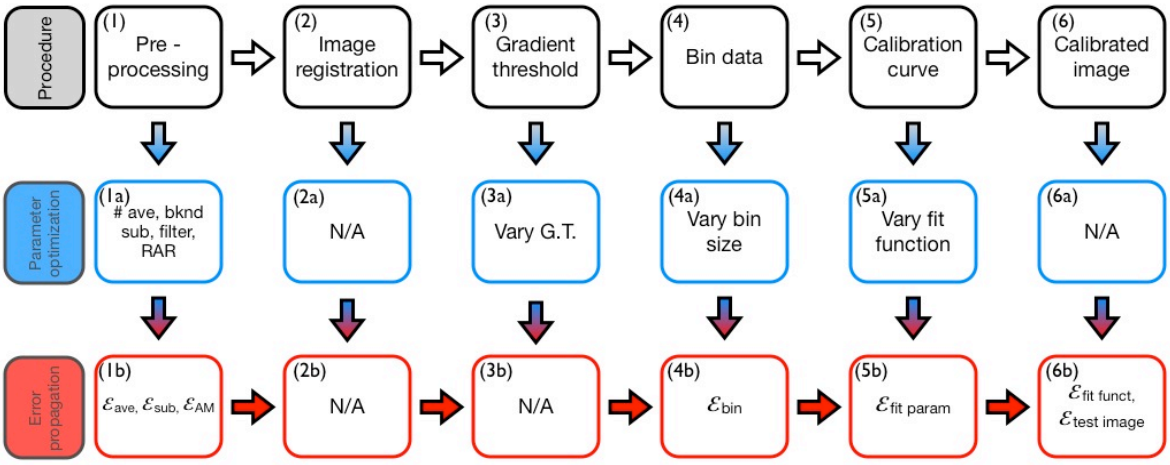

Figure 3. PGD CT image processing procedure with associated optimization parameters and errors. Red right-pointing arrows indicate an error propagation step. Taken from Jirasek *et al* 2014 with permission from Jirasek *et al* 2012.

5. Conclusions

Polymer gel dosimetry remains one of the most promising tools for measuring inherently complex 3D radiotherapy dose distributions. In fact, polymer gel dosimetry is currently feasible with MRI-based dose readout. However, the uncertainties within a given polymer gel system, irrespective of the imaging modality used to extract dose information, are non-trivial in nature and great care is required in understanding the magnitudes of errors and uncertainties within a full gel dosimetry protocol. With every dosimeter and imaging modality it is crucial to follow a careful optimized protocol and compensate for imaging artefacts to minimize the uncertainties. This review poses points for consideration when undertaking a benchmarking of accuracy and precision of polymer gel dosimetry imaged with MRI, optical or x-ray CT.

6. References

[1] Baldock C *et al* 2010 *Phys. Med. Biol.* **55** R1-63
[2] Vergote K *et al* 2004 *Phys. Med. Biol.* **49** 287-305
[3] De Deene Y *et al* 2000 *Magn. Reson. Med.* **43** 116-25
[4] Dumas E *et al* 2006 *J. Phys.: Conf. Ser.* **56** 239-41
[5] MacDougall N D *et al* 2008 *Br. J. Radiol.* **81** 46-50
[6] De Deene Y *et al* 2007 *Phys. Med. Biol.* **52** 2719-28
[7] Cosgrove V P *et al* 2000 *Phys. Med. Biol.* **45** 1195-210
[8] Sedaghat M *et al* 2011 *Phys. Med. Biol.* **56** 6083-107
[9] Hilts M *et al* 2000 *Phys. Med. Biol.* **45** 2559–71
[10] Audet C *et al* 2002 *J. Phys.: Conf. Ser.* **3** pp. 110-18
[11] Jirasek A and Hilts M *et al* 2014 *Phys. Med. Biol.* **59** 597-614
[12] Johnston H *et al* 2012 *Phys. Med. Biol.* **57** 3155-75
[13] Low D A 2010 *J. Phys.: Conf. Ser.* **250** 012071
[14] De Deene Y *et al* 1998 *Radiother. Oncol.* **48** 283-91
[15] Haraldsson P *et al* 2000 *Br. J. Radiol.* **73** 58-65
[16] Pappas E *et al* 2001 *Phys. Med. Biol.* **46** 783-97
[17] Ibbott G S *et al* 1997 *Int. J. Radiat. Oncol. Biol. Phys.* **38** 1097-103
[18] Oldham M *et al* 1998 *Phys. Med. Biol.* **43** 1113-32
[19] Meeks S L *et al* 1999 *Int. J. Radiat. Oncol. Biol. Phys.* **43** 1141-53

[20] Cosgrove V P *et al* 2000 *Phys. Med. Biol.* **45** 1195-210
[21] Ramm U *et al* 2000 *Phys. Med. Biol.* **45** N95-102
[22] Farajollahi A R *et al* 2000 *Phys. Med. Biol.* **45** N9-14
[23] Grebe G *et al* 2001 *Int. J. Radiat. Oncol. Biol. Phys.* **49** 1451-60
[24] De Deene Y 2006 *J. Phys.: Conf. Ser.* **56** 72-85
[25] Low D A *Med. Phys.* **25** 656-61
[26] Jiang S B *et al* 2006 *Phys. Med. Biol.* **51** 759-76
[27] Vandecasteele J and De Deene Y 2013 *Phys. Med. Biol.* **58** 19-42
[28] Meeks S L *et al* 1999 *Int. J. Radiat. Oncology Biol. Phys.* **43** 1135-41
[29] De Deene Y *et al* 2006 *Phys. Med. Biol.* **51** 653-73
[30] Salomons G J *et al* 2002 *Phys. Med. Biol.* **47** 1435-48
[31] Karlsson A *et al* 2007 *Phys. Med. Biol.* **52** 4697-706
[32] De Deene Y *et al* 2002 *Phys. Med. Biol.* **47** 2459-70
[33] Vergote K *et al* 2004 *Phys. Med. Biol.* **49** 4507-22
[34] De Deene Y *et al* 1998 *Signal Processing* **70** 85-101
[35] De Deene Y and Baldock C 2002 *Phys. Med. Biol.* **47** 3117-41
[36] Hilts M *et al* 2005 *Phys. Med. Biol.* **50** 1727-45
[37] De Deene Y and Vandecasteele J 2013 *J. Phys.: Conf. Ser.* **444** 012015
[38] Vandecasteele J and De Deene Y 2013 *Phys. Med. Biol.* **58** 43-61
[39] Vandecasteele J and De Deene Y 2013 *Phys. Med. Biol.* **58** 63-85
[40] De Deene Y 2004 *J. Phys.: Conf. Ser.* **3** 87-114
[41] De Deene Y 2009 *J. Phys.: Conf. Ser.* **164** 012033
[42] De Deene Y *et al* 2000 *Phys. Med. Biol.* **45** 1807-23
[43] De Deene Y *et al* 2000 *Phys. Med. Biol.* **45** 1825-39
[44] De Deene Y and De Wagter C 2001 *Phys. Med. Biol.* **46** 2697-711
[45] Doran S J *et al* 2005 *Phys. Med. Biol.* **50** 1343-61
[46] De Deene Y *et al* 2001 *Phys. Med. Biol.* **46** 2801-25
[47] De Deene Y 2010 *J. Phys.: Conf. Ser.* **250** 012015
[48] Doran S J and Krstajic N 2006 *J. Phys.: Conf. Ser.* **56** 45-57
[49] Gore J C *et al* 1996 *Phys. Med. Biol.* **41** 2695-704
[50] Cheng H-W *et al* 2011 *Radiat. Meas.* **46** 1932-5
[51] Campbell W G *et al Med. Phys.* **40** 061712-1-12
[52] Doran S J *et al* 2001 *Phys. Med. Biol.* **46** 3191-213
[53] Krstajic N and Doran S J 2007 *Phys. Med. Biol.* **52** N257-63
[54] Lopatiuk-Tirpak O *et al* 2008 *Med. Phys.* **35** 3847-59
[55] Maryanski M J and Ranade M K 2001 *Proc. SPIE* **4320** 764-74
[56] Olding T *et al* 2010 *Phys. Med. Biol.* **55** 2819-40
[57] Ramm D *et al* 2012 *Phys. Med. Biol.* **57** 3853-68
[58] Vandecasteele J and De Deene Y 2009 *J. Phys.: Conf. Ser.* **56** 45-57
[59] Xu Y and Wuu C-S 2013 *Phys Med Biol* **58** 479-95
[60] Sakhalkar H S and Oldham M 2008 *Med. Phys.* **35** 101-11
[61] Jordan K and Avvakumov N 2009 *Phys. Med. Biol.* **54** 6773-89
[62] Vandecasteele J and De Deene Y 2013 *Phys. Med. Biol.* **58** 6241-62
[63] Skyt P S *et al* 2012 *Med Phys* **39** 7232
[64] Guo P Y *et al* 2006 *Med. Phys.* **33** 1338-45
[65] Yates E S *et al* 2011 *Acta Oncologica* **50** 829-34
[66] De Deene Y et al 2014 Proceedings of 8th International Conference on 3D Radiation Dosimetry (IC3DDose) 4-7 September 2014, Ystad, Sweden
[67] Krstajic N and Doran S 2007 *Phys. Med. Biol.* **52** 3693-713
[68] De Deene Y 2014 Proceedings of 8th International Conference on 3D Radiation Dosimetry (IC3DDose) 4-7 September 2014, Ystad, Sweden

[69] Bosi S G *et al* 2009 *Phys. Med. Biol.* **54** 275-83.
[70] Skyt P S *et al* 2012 *Med Phys* **39** 7232-6
[71] Oldham M and Kim L 2004 *Med. Phys.* **31** 1093-104
[72] Xu Y *et al* 2004, *Med. Phys.* **31** 3024-33
[73] Oldham M *et al* 2003 *Med. Phys.* **30** 623-34
[74] Xu Y *et al* 2010 *Med. Phys.* **37** 861-8
[75] Alwan R *et al* 2008 *Nucl. Instr. Meth. Phys. Research B* **266** 834-40
[76] Doran S J 2010 *J. Phys.: Conf. Ser.* **250** 012086